Search for neutrinoless double beta decay with enriched ^{76}Ge in Gran Sasso 1990–2003

H.V. Klapdor-Kleingrothaus [*],[1], I.V. Krivosheina [2], A. Dietz, O. Chkvorets

Max-Planck-Institut für Kernphysik, PO 10 39 80, D-69029 Heidelberg, Germany

Abstract

The results of the HEIDELBERG–MOSCOW experiment which searches with 11 kg of enriched ^{76}Ge for double beta decay in the Gran Sasso underground laboratory are presented for the full running period August 1990–May 2003. The duty cycle of the experiment was ∼80%, the collected statistics is 71.7 kg yr. The background achieved in the energy region of the Q value for double beta decay is 0.11 events kg^{-1} yr^{-1} keV^{-1}. The two-neutrino accompanied half-life is determined on the basis of more than 100 000 events. The confidence level for the neutrinoless signal has been improved to 4.2σ.
© 2004 Elsevier B.V. All rights reserved.

1. Introduction

Since 40 years large experimental efforts have gone into the investigation of nuclear double beta decay which probably is the most sensitive way to look for (total) lepton number violation and probably the only way to decide the Dirac or Majorana nature of the neutrino. It has further perspectives to probe also other types of beyond standard model physics. This thorny way has been documented recently in some detail [1].

The half-lives to explore lying, with the order of 10^{25} years, in a range on 'half way' to that of proton decay, the two main experimental problems were to achieve a sufficient amount of double beta emitter material (source strength) and to reduce the background in such experiment to an extremely low level. The final dream behind all these efforts was less to see a standard-model allowed second-order effect of the weak interaction in the nucleus—the two-neutrino-accompanied decay mode—which has been observed meanwhile for about ten nuclei—but to see neutrinoless double beta decay, and with this a first hint of beyond standard model physics, yielding at the same time a solution of the absolute scale of the neutrino mass spectrum.

In this Letter we describe the HEIDELBERG–MOSCOW experiment, which was proposed in 1987 [2], and which started operation in the Gran Sasso Underground Laboratory with the first detector in 1990.

[*] Corresponding author.
E-mail address: klapdor@gustav.mpi-hd.mpg.de
(H.V. Klapdor-Kleingrothaus).
URL: http://www.mpi-hd.mpg.de.non_acc/.
[1] Spokesman of HEIDELBERG–MOSCOW (and GENIUS) Collaboration.
[2] On leave of the Radiophysical Research Institute, Nishnii-Novgorod, Russia.

We report the result of the measurements over the full period August 1990 until May 2003 (the experiment is still running, at the time of submission of this Letter). The quality of the new data and of the present analysis, which has been improved in various respects, allowed us to significantly improve the investigation of the neutrinoless double beta decay process, and to deduce more stringent values on its parameters.

We are giving in a detailed paper [3] (for earlier papers see [4,5]) a full description of the experimental procedure, the specific features and challenges of the data acquisition and background reduction. In this Letter we mainly present the data, taken with a total statistics of 71.7 kg yr for the period August 2, 1990–May 20, 2003, and we present their analysis.

2. Experimental parameters

The HEIDELBERG–MOSCOW experiment is, with five enriched to 86–88% high-purity p-type Germanium detectors, of in total 10.96 kg of active volume, using the largest source strength of all double beta experiments at present, and has reached a record low level of background. It is since ten years now the most sensitive double beta decay experiment worldwide. The detectors were the first *high-purity* Ge detectors ever produced. The degree of enrichment has been checked by investigation of tiny pieces of Ge *after* crystal production using the Heidelberg MP-Tandem accelerator as a mass spectrometer. Since 2001 the experiment has been operated only by the Heidelberg group, which also performed the analysis of the experiment from its very beginning.

We start by listing up some of the most essential features of the experiment.

(1) Since the sensitivity for the $0\nu\beta\beta$ half-life is $T_{1/2}^{0\nu} \sim a\epsilon\sqrt{Mt/\Delta E B}$ (and $1/\sqrt{T^{0\nu}} \sim \langle m_\nu \rangle$), with a denoting the degree of enrichment, ϵ the efficiency of the detector for detection of a double beta event, M the detector (source) mass, ΔE the energy resolution, B the background and t the measuring time, the sensitivity of our 11 kg *of enriched* ^{76}Ge experiment corresponds to that of an at least 1.2 ton *natural* Ge experiment. After enrichment—the other most important parameters of a $\beta\beta$ experiment are: energy resolution, background and source strength.

(2) The high energy resolution of the Ge detectors of 0.2% or better, assures that there is no background for a $0\nu\beta\beta$ line from the two-neutrino double beta decay in this experiment (5.5×10^{-9} events expected in the energy range 2035–2039.1 keV), in contrast to most other present experimental approaches, where limited energy resolution is a severe drawback.

(3) The efficiency of Ge detectors for detection of $0\nu\beta\beta$ decay events is close to 100% (95%, see [6](a)).

(4) The source strength in this experiment of 11 kg is the largest source strength ever operated in a double beta decay experiment.

(5) The background reached in this experiment, is 0.113 ± 0.007 events kg^{-1} yr^{-1} keV^{-1} (in the period 1995–2003) in the $0\nu\beta\beta$ decay region (around $Q_{\beta\beta}$). This is the lowest limit ever obtained in such type of experiment.

(6) The statistics collected in this experiment during 13 years of stable running is the largest ever collected in a double beta decay experiment. The experiment took data during ∼80% of its installation time.

(7) The Q value for neutrinoless double beta decay has been determined recently with high precision [7,8].

3. Background of the experiment

The background of the experiment consists of

(1) Primordial activities of the natural decay chains from ^{238}U, ^{232}Th, and ^{40}K;

(2) Anthropogenic radio nuclides, like ^{137}Cs, ^{134}Cs, ^{125}Sb, ^{207}Bi;

(3) Cosmogenic isotopes, produced by activation due to cosmic rays during production and transport;

(4) The bremsstrahlungs spectrum of ^{210}Bi (daughter of ^{210}Pb);

(5) Elastic and inelastic neutron scattering, and

(6) Direct muon-induced events.

The detectors, except detector No. 4, are operated in a common Pb shielding of 30 cm, which consists of an inner shielding of 10 cm radiopure LC2-grade Pb followed by 20 cm of Boliden Pb. The whole setup is placed in an air-tight steel box and flushed with radiopure nitrogen in order to suppress the ^{222}Rn

contamination of the air. The shielding has been improved in the course of the measurement. The steel box is since 1994 centered inside a 10-cm boron-loaded polyethylene shielding to decrease the neutron flux from outside. An active anticoincidence shielding is placed on the top of the setup since 1995 to reduce the effect of muons. Detector No. 4 is installed in a separate setup, which has an inner shielding of 27.5 cm electrolytical Cu, 20 cm lead, and boron-loaded polyethylene shielding below the steel box, but no muon shielding.

The setup has been kept hermetically closed since installation of detector 5 in February 1995. Since then no radioactive contaminations of the inner of the experimental setup by air and dust from the tunnel could occur.

A detailed description of the remaining background, and corresponding Monte Carlo simulations with GEANT4 are given in [9]. Important result is, that there are no background γ-lines to be expected at the position of an expected $0\nu\beta\beta$ line, according to this Monte Carlo analysis of radioactive impurities in the experimental setup [9] and according to the compilations in [10]. Some γ-peaks in the simulated spectrum near $Q_{\beta\beta}$ are emitted from the isotope ^{214}Bi. So from ^{214}Bi (^{238}U-decay chain) in the vicinity of the Q-value of the double beta decay of $Q_{\beta\beta} = 2039$ keV, according to the Table of Isotopes [10], weak lines should be expected at 2010.7, 2016.7, 2021.8 and 2052.9 keV (see [11]). It should be especially noted, that also neutron capture reactions ^{74}Ge$(n,\gamma)^{75}$Ge and ^{76}Ge$(n,\gamma)^{77}$Ge and subsequent radioactive decay have been simulated by GEANT4 in [9]. The simulation yields, in the range of the spectrum 1990–2110 keV, for the total contribution from decay of ^{77}Ge 0.15 counts. So in particular, the 2037.8 keV transition in the γ-decay following β^- decay of ^{77}Ge [10] is not expected to be seen in the measured spectra. It would always be accompanied by a 10 times stronger line at 2000.1 keV [10], which is not seen in the spectrum (Figs. 3, 4).

4. Control of stability of the experiment and data taking

To control the stability of the experiment, a calibration with a ^{228}Th and a ^{152}Eu + ^{228}Th source, has been done weekly. High voltage of the detectors, temperature in the detector cave and the computer room, the nitrogen flow flushing the detector boxes to remove radon, the muon anticoincidence signal, leakage current of the detectors, overall and individual trigger rates are monitored daily. The energy spectrum is taken in parallel in 8192 channels in the range from threshold up to about 3 MeV, and in a spectrum up to about 8 MeV. Data taking since November 1995 is done by a CAMAC system, and CETIA processor in event by event mode. To read out the used 250 MHz flash ADCs of type Analog Devices 9038 JE (in DL515 modules), which allow digital measurement of pulse shapes for the four largest detectors (for later off-line analysis), a data acquisition system on VME basis has been developed [6](c). The resolution of the FADCs is 8 bit, and thus not sufficient for a measurement of energies. The energy signals for high and low-energy spectra are recorded with 13 bit ADCs developed at MPI Heidelberg. The acquisition system used *until* 1995 (VAX/VMS) did not allow to measure the pulse shapes of all detectors because of the too low data transfer rates. For the period 1990–1995 we prepared the final sum spectrum taken with the former electronics shortly after this measuring period, setting the proper conditions for data acceptance [6](a,b,c). Since 1995, in total we have taken with the since then new electronics, 2142 runs (10 513 data sets for the five detectors) (*without* calibration measurements), the average length of which was about one day. From these raw data runs and data sets only those are considered for further analysis which fulfill the following conditions:

(1) No coincidence with another Ge detector;
(2) No coincidence with plastic scintillator (muon shield);
(3) No deviation from average count rate of each detector more than $\pm5\sigma$;
(4) Only pulses with ratios of the energy determined in the spectroscopy branch, and the area under the pulse detected in the *timing* branch (EoI values [12]), within a $\pm3\sigma$ range around the mean value for each detector are accepted;
(5) We ignore for each detector the first 200 days of operation, corresponding to about three half-lifes of ^{56}Co ($T_{1/2}^{0\nu} = 77.27$ days), to allow for decay of short-lived radioactive impurities;

Table 1

Collected statistics and background numbers in the different data acquisition periods for the enriched detectors of the HEIDELBERG–MOSCOW experiment for the period 1990–2003

Detector No.	Life time accepted (days)	Date Start End	Background[a]	PSA	Life time accepted (days)	Date Start End	Background[a]	PSA
1	930.9	8/90–8/95	0.31	no	2090.61	11/95–5/03	0.20	no
2	997.2	9/91–8/95	0.21	no	1894.11	11/95–5/03	0.11	yes
3	753.1	9/92–8/95	0.20	no	2079.46	11/95–5/03	0.17	yes
4	61.0	1/95–8/95	0.43	no	1384.69	11/95–5/03	0.21	yes
5	–	12/94–8/95	0.23	no	2076.34	11/95–5/03	0.17	yes
	Over period 1990–1995				Over period 1995–2003			
	Accepted life time = 15.05 kg yr				Accepted life time = 56.655 kg yr			

[a] Background determined by averaging counting rate in interval 2000–2100 keV (counts keV^{-1} yr^{-1} kg^{-1}); background determined from 11.1995 till 05.2003 at $Q_{\beta\beta}$ from *fit* of spectrum in range 2000–2060 keV is (0.113 ± 0.007) events keV^{-1} yr^{-1} kg^{-1} (all numbers without PSA).

(6) ADCs or other electronics units were working properly (corrupted data are excluded).

From the totally registered 951 044 events in the spectrum measured since 1995, there remain finally 786 652 events (9570 data sets). From these we find in the range 2000 to 2060 keV around $Q_{\beta\beta}$—562 events.

5. *Q* value

The expectation for a $0\nu\beta\beta$ signal would be a sharp line at the Q value of the process. Earlier measurements gave $Q_{\beta\beta} = (2040.71 \pm 0.52)$ keV, (2038.56 ± 0.32) keV and (2038.668 ± 2.142) keV [8]. The recent precision measurement of [7] gave a value of (2039.006 ± 0.050) keV.

6. **Development of the experiment**

Table 1 shows the collected statistics of the experimental setup and of the background number in the different data acquisition periods for the five enriched detectors of the experiment for the total measuring time August 1990 to May 2003.

7. **Reliability of data acquisition and data**

We have carefully checked all data before starting the analysis. For details we refer to [3]. We checked the proper operation of the thresholds in all ADCs. Fig. 1 shows the threshold ranges for detectors 4

and 5, from the list mode data acquisition of the measurement, for the data used in the analysis. The effect discussed in [13] (their Fig. 4) is not present in our analysis. Also the other effects discussed in [13] are not present in the analysis. A detailed analysis shows that these effects arise from including corrupt data into the analysis (see also [3]).

The stability of the experiment over the years and of the energy resolution and calibration is demonstrated in the following figures for the two ^{228}Th lines used for calibration in the range of $Q_{\beta\beta}$: Fig. 1 (right) shows the *sum* of all weekly calibration spectra (∼360 *spectra* for *each* detector) for the 2614.5 keV Th line. Fig. 2 (left) shows the resolution and energy position after *summing* the spectra *of the five detectors* (∼1800 *spectra*). The integrated resolution over 8 years of measurement is found to be 3.27 keV, i.e., better than in our earlier analysis of the data until May 2000 [14, 15]. This is a consequence also of the refined summing procedure we used for the individual 9 570 data sets.

Fig. 2 (right) shows as another example the *sum* of all weekly calibration spectra for the 2103.5 keV line for each detector. The agreement of the energy positions for the different detectors is seen to be very good.

We also checked the arrival time distribution of the events, and proved that this is not affected by any technical operation during the measurement, such as the calibration procedure (introducing the Th source into the detector chamber through a thin tube) and simultaneously refilling of liquid nitrogen to the detectors, etc. No hint is seen for introduction of any radioac-
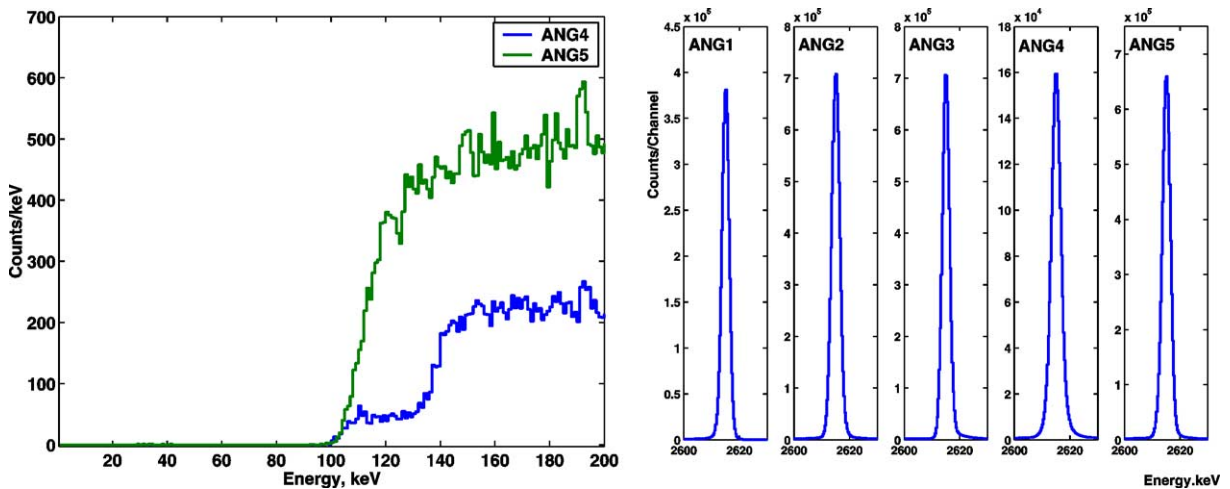
Fig. 1. Left: Threshold ranges for detectors 4 and 5 in the spectrum measured during 1995–2003. Right: *Sum* of the (∼360) weekly calibration spectra for the 2614.5 keV line from [228]Th over the measuring time 1995–2003.
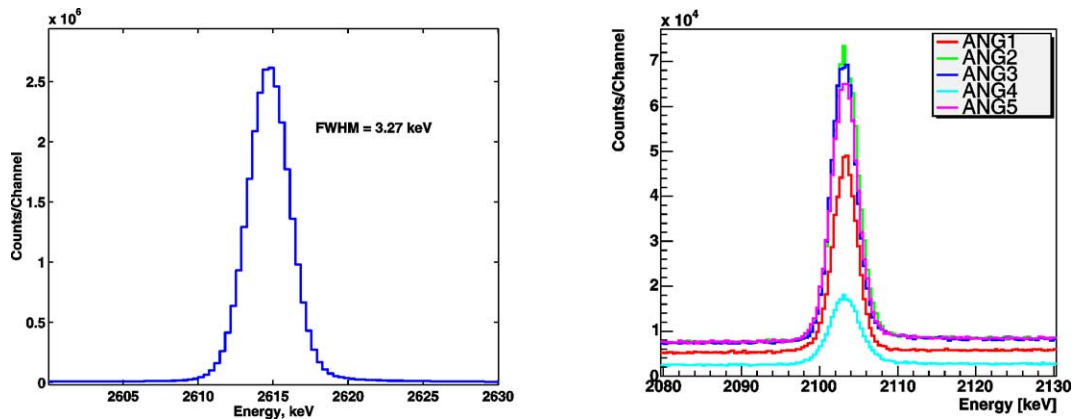

Fig. 2. Left: Sum of the sum of the weekly calibration spectra of all five detectors shown in Fig. 1 (right) (∼1800 spectra). Right: Sum of calibration spectra for each detector (absolute intensities) for the 2103.5 keV line for the period 1995–2003 (from top to bottom detectors: 2, 3, 5, 1, 4).

tive material from the exterior. The measured distribution corresponds to a uniform distribution in time on a 99% c.l. [3]. This has been proven by a Kolmogorov–Smirnov goodness-of-fit test.

8. Data and analysis

Fig. 3 shows the total sum spectrum measured over the full energy range of all five detectors for the period August 1990 to May 2003. All identified lines are indicated with their source of origin (for details see [6,9](e,f)).

In the measured spectra (Fig. 4) we see in the range *around* $Q_{\beta\beta}$ the [214]Bi lines at 2010.7, 2016.7, 2021.8, 2052.9 keV, a line at $Q_{\beta\beta}$ and a candidate of a line at ∼2030 keV (the latter could originate, as mentioned in [11,16], from electron conversion of the 2118 keV γ-line from [114]Bi. On the other hand, as noted in [16], its energy differs from $Q_{\beta\beta}$ just by the K-shell X-ray energies of Ge(Se) of 9.2(10.5) keV). We show the energy range 2000–2060 keV, since here a simultaneous fit can be made to safely attributed lines (except the 2030 keV line), in contrast to the range we used earlier (2000–2100 keV). *Non-integer*
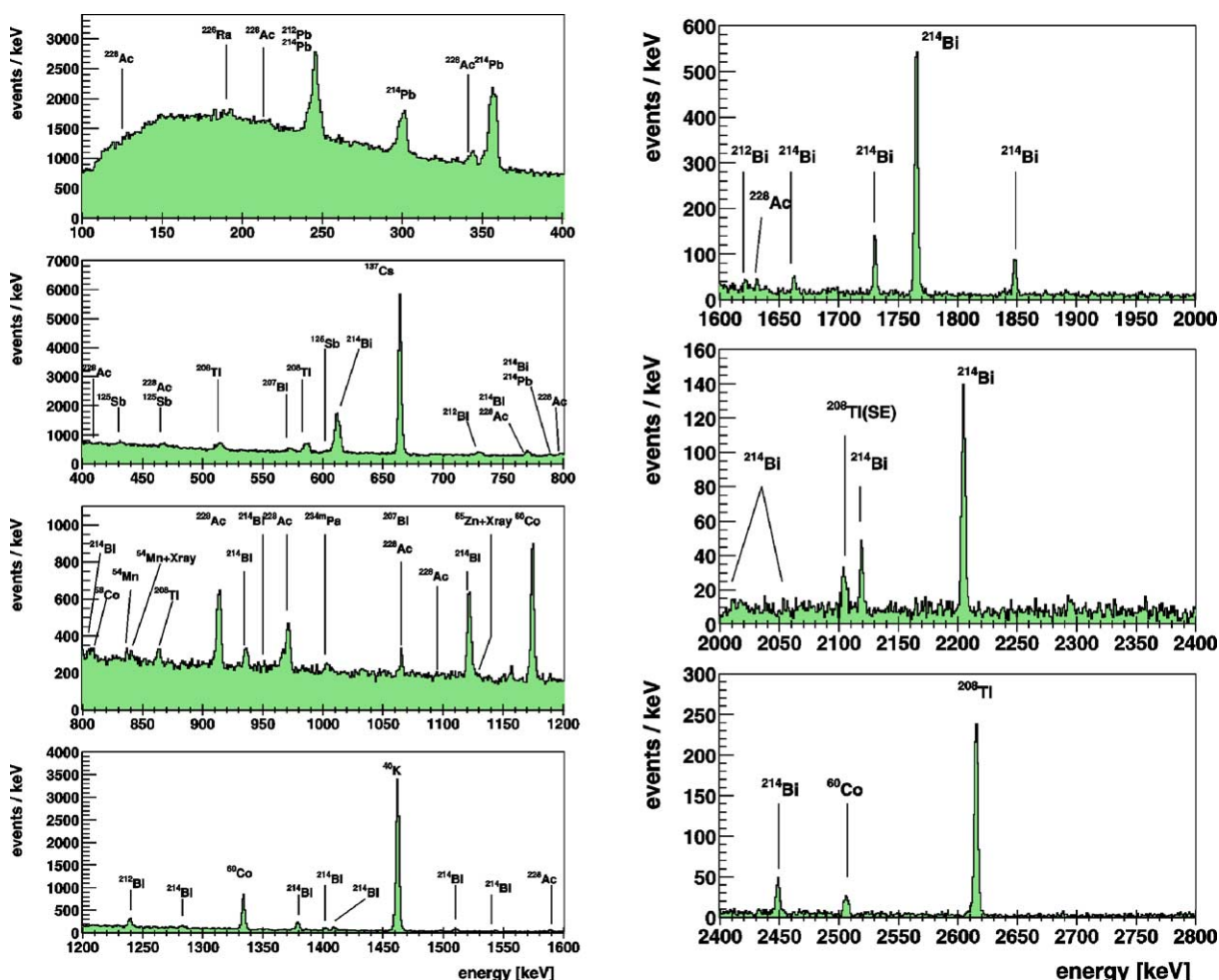
Fig. 3. The total sum spectrum measured over the full energy range with all five detectors (in total 10.96 kg enriched in ^{76}Ge to 86%) for the period from August 1990 to May 2003.

numbers in the sum spectra are simply a binning effect. While a peak-search procedure as shown in Fig. 4 (bottom right) was needed earlier, to project out the lines from the spectrum [14,15], they can now, with more statistics and improved analysis, be directly clearly seen in the spectra. The large improvement of the present analysis compared to our paper from 2001 [14], is clearly seen from Fig. 4 (top left) showing the *new* analysis of the data 1990–2000, as performed here—to be compared to the corresponding figure in [14,15]. One reason is, that the stricter conditions for accepting data into the analysis, in particular, of conditions (4) and (6) in Section 4,

cleaned the spectrum considerably. The spectrum in Fig. 4 (top left) now corresponds to 50.57 kg yr to be compared to 54.98 kg yr in [14], for the same measuring period. The second reason is a better energy calibration of the individual runs. The third reason is the refined summing procedure of the individual data sets mentioned above and the correspondingly better energy resolution of the final spectrum. (For more details see [3].) The signal strength seen in the *individual* detectors in the period 1995–2003 is shown in Fig. 5. When adding the spectra of Fig. 5 for two subsets of detectors, detectors $1 + 2 + 4$, and $3 + 5$, both resulting spectra already clearly indicate, in
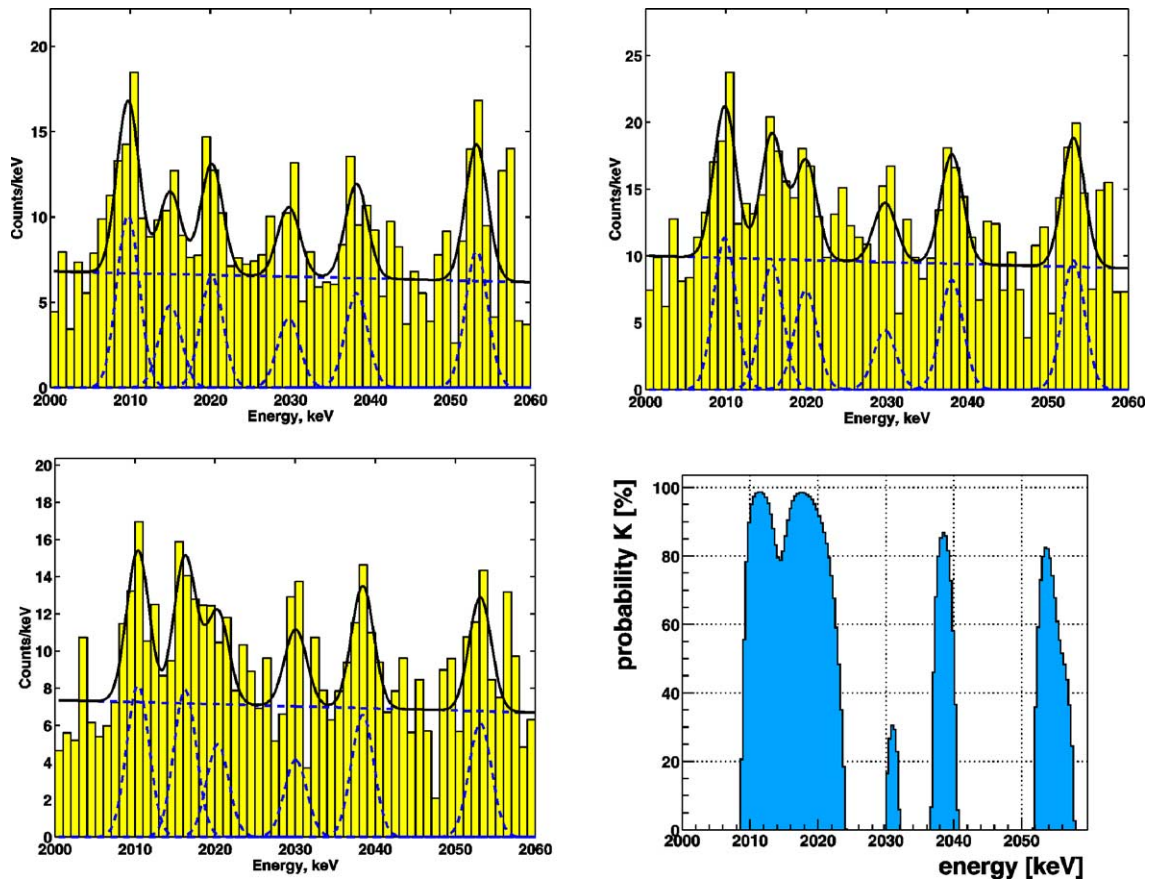
Fig. 4. The total sum spectrum of all five detectors (in total 10.96 kg enriched in ^{76}Ge), in the range 2000–2060 keV and its fit, for the periods: Top: left—August 1990 to May 2000 (50.57 kg yr); right—August 1990 to May 2003 (71.7 kg yr). Bottom: left—November 1995 to May 2003 (56.66 kg yr); right—scan for lines in the spectrum shown on the left, with the MLM method (see text). The Bi lines at 2010.7, 2016.7, 2021.8 and 2052.9 keV are seen, and in addition a signal at ∼2039 keV.

contradiction to a claim of [13], the signal at $Q_{\beta\beta}$ (see Fig. 6 and Table 2). The time distribution of the events throughout the measuring time and the distribution among the detectors corresponds to the expectation for a constant rate, and to the masses of the detectors (see Fig. 7).

The spectra have been analyzed by *different methods*: Least Squares Method, Maximum Likelihood Method (MLM) and Feldman–Cousins Method. The analysis is performed *without subtraction of any background*. We always process background-plus-signal data since the difference between two Poissonian variables does *not* produce a Poissonian distribution [17]. This point is sometimes overlooked. So, e.g., in [18] a formula is developed making use of such subtraction

and as a consequence the analysis given in [18] provides overestimated standard errors.

We have performed first a simultaneous fit of the range 2000–2060 keV of the measured spectra by the nonlinear least squares method, using the Levenberg–Marquardt algorithm [19]. It is applicable in *any* statistics [20] under the following conditions: (1) relative errors asymptotic to zero, (2) ratio of signal to background asymptotic constant. It does not require exact knowledge of the probability density function of the data.

We fitted the spectra using *n* Gaussians (*n* is equal to the number of lines, which we want to fit) $G(E_i, E_j, \sigma_j)$ and using different background models $B(E_i)$: simulated background (linear with fixed slope)
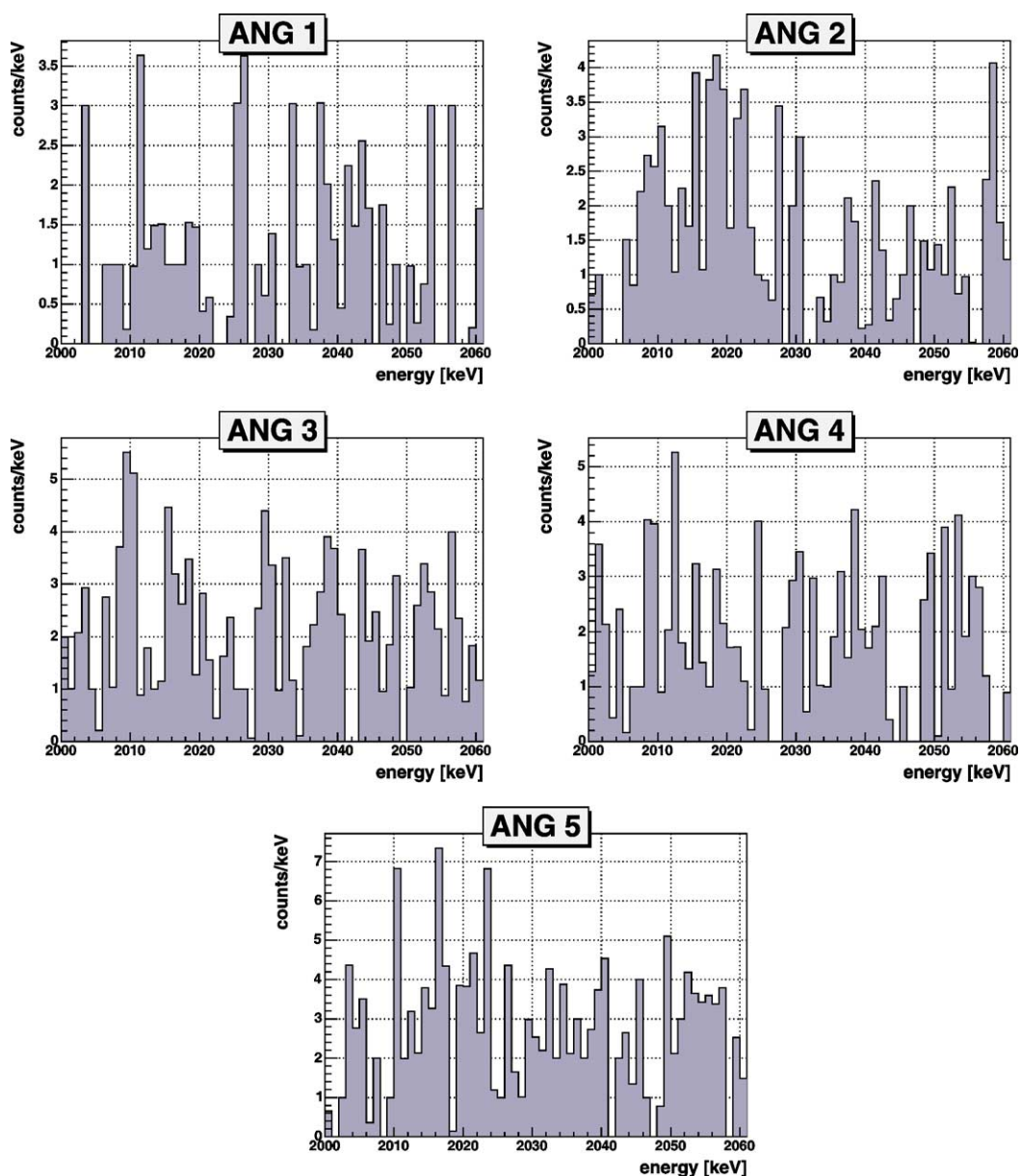
Fig. 5. The spectra of the individual five detectors in the range 2000–2060 keV for the period from November 1995 to May 2003. The sum corresponds to the spectrum shown in Fig. 4, bottom left.

(see [9]), linear, and constant. The fitting function $F(E_i)$ thus is a sum of Gaussians and background.

Error estimate: the Levenberg–Marquardt method [19] is one of the most tested minimization algorithms, finding fits most directly and efficiently. It also is reasonably insensitive to the starting values of the pa-

rameters. This method has advantages over others of providing an estimate of the full error matrix. The MATLAB Statistical Toolbox [21] provides functions for confidence interval estimation for all parameters. We tested the confidence intervals calculated by the MATLAB statistical functions with numerical simu-
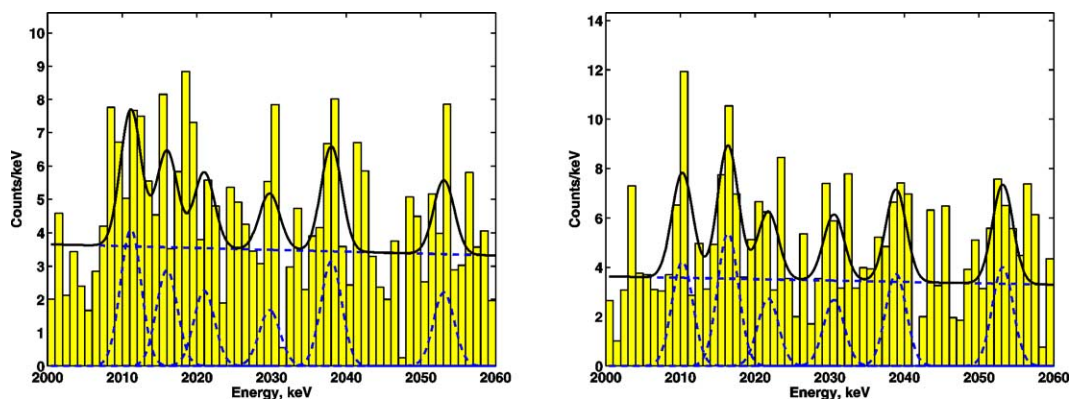
Fig. 6. Spectra measured with detectors $1 + 2 + 4$ (left part), detectors $3 + 5$ (right part) over the period 1995–2003. The sum of the spectra is equal to that shown in Fig. 4 (bottom left).
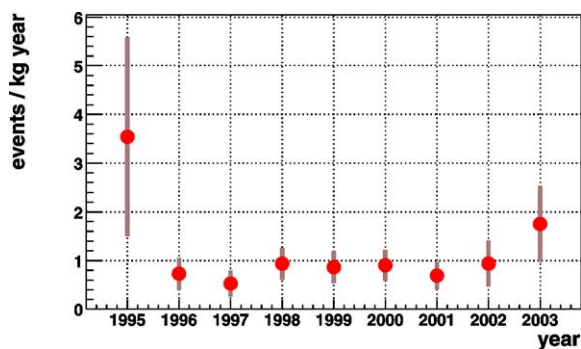

Fig. 7. The measured *total* counting rates in the period from November 1995 to May 2003 in the energy range 2036.5–2041.0 keV as function of time (1σ statistical errors are given).

lations. As done earlier for other statistical methods [15], we have simulated samples of 100 000 spectra each, with Poisson-distributed background and a Gaussian-shaped (Poisson-distributed) line of given intensity, and have investigated, in how many cases we find in the analysis the known intensities inside the given confidence range (for details see [3]). We find the confidence levels calculated by this method to be correct within $\sim 0.3\sigma$. The second standard method, we have used to analyze the measured spectra, is the Maximum Likelihood Method (MLM) using the root package from CERN [22], which exploits the program MINUIT for error calculation. For this purpose the program provided there had to be extended for application to non-integer numbers (for details see [23]). We performed also in this case a test of the given confidence intervals given by this program, by numerical

simulations. Taking into account the results, the application of the MLM yields results for the confidence levels consistent with the Least Squares Method. The third method used for analysis is the Feldman–Cousins–Method (FCM) described in detail in [24].

9. Results

Fig. 4 shows together with the measured spectra in the range around $Q_{\beta\beta}$ (2000–2060 keV), the fits using the first of the methods described. In these fits a linear decreasing shape of the background as function of energy was chosen, corresponding to the complete simulation of the background performed in [9] by GEANT4. In these fits the peak positions, widths and intensities are determined simultaneously, and also the *absolute* level of the background. E.g., in Fig. 4 (middle), the *fitted* background corresponds to (55.94 ± 3.92) kg yr if extrapolated from the background *simulated* in [9] for the measurement with 49.59 kg yr of statistics. This is almost *exactly* the statistical significance of the present experiment (56.66 kg yr) and thus a nice proof of consistency.

For the line near $Q_{\beta\beta}$ we obtain for the measuring periods 1990–2003 (1995–2003) the following result: energy (in keV) 2038.07 ± 0.44 (2038.44 ± 0.45), intensity 28.75 ± 6.86 (23.04 ± 5.66) events. This result is obtained assuming the linearly decreasing background as described. Assuming a *constant* background in the range 2000–2060 keV or keeping also the *slope* of a linearly varying background as a free parameter, yields very similar results. For the analysis of the other
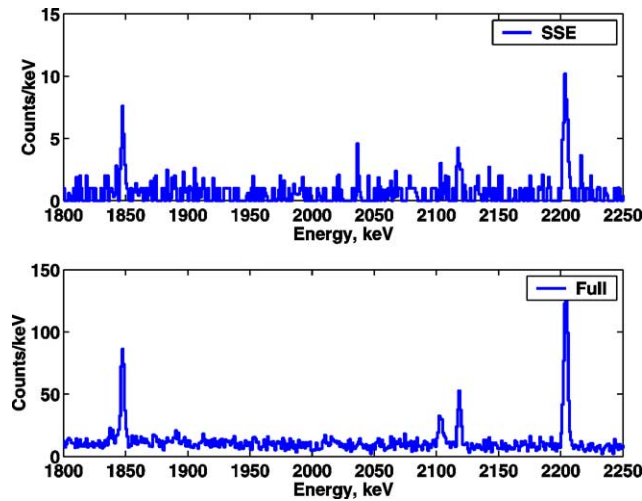
Fig. 8. The pulse-shape selected (above) and the full (below) spectrum measured with detectors 2, 3, 4, 5 from 1995–2003, in the energy range 1800–2250 keV.

lines we refer to [3]. For the period 1990–2000 (see Fig. 4) we obtain an intensity of 19.36 ± 6.22 events, consistent with the 14.8 events reported in [14,15] for 46.5 kg yr. The signal at ~ 2039 keV in the full spectrum thus reaches a 4.2σ confidence level for the period 1990–2003, and of 4.1σ for the period 1995–2003. We have given a detailed comparison of the spectrum measured in this experiment with other Ge experiments in [16]. It is found that the most sensitive experiment with natural Ge detectors [25], and the first experiment using enriched (not yet high-purity) ^{76}Ge detectors [26] find essentially the same background lines (^{214}Bi, etc.), but *no* indication for the line near $Q_{\beta\beta}$.

The fits obtained with the Maximum Likelihood Method agree with the results, given above. The estimations of the Feldman–Cousins Method yield confidence levels for the line at $Q_{\beta\beta}$ at a $\sim 4\sigma$ level. The uncertainty in the determination of the background here is larger, than in a consistent fit of the full range of interest by the other two methods.

10. Time structure of events

We developed for the HEIDELBERG–MOSCOW experiment some *additional tool* of independent verification, whose present status will be presented here briefly. The method is to exploit the time structure of

the events and to select $\beta\beta$ events by their pulse shape. Applying a method similar to that described earlier [15], accepting only events as single site events (SSE), classified by one of the neuronal net methods [12], and in most cases simultaneously also by the second and third method [12] mentioned in [15], as SSE (for details see [23]), we find a 3.3σ signal for the line near $Q_{\beta\beta}$ (12.36 ± 3.72 events), and we find the other lines, at 2010.7, 2016.7 and 2021.8 keV to be consistent in intensity with *normal* γ-lines, i.e., considerably more reduced (see [3]). When calibrating the pulse shape analysis method with the 1592 keV double escape line from ^{228}Th source—assuming that the $0\nu\beta\beta$ events behave like the single site events in a double escape line—it can be concluded that the line at $Q_{\beta\beta}$ is consisting of SSE (for details see [3]).

That a neuronal net method selection of the specific pulse shapes created by double beta decay can be done with much higher sensitivity, can be seen from Fig. 8. Here a defined subclass of the shapes selected above is selected, corresponding to events in part of the inner volume of the detectors. Except a line which sticks out sharply near $Q_{\beta\beta}$, *all* other lines are very strongly suppressed. The probability to find ~ 7 events in two neighboring channels from background fluctuations is calculated to be 0.013%. Thus, we see a line near $Q_{\beta\beta}$ at a 3.8σ level. This method also fulfills the criterium to select properly the *continuous $2\nu\beta\beta$ spectrum* (see Fig. 9), which *is not* done properly
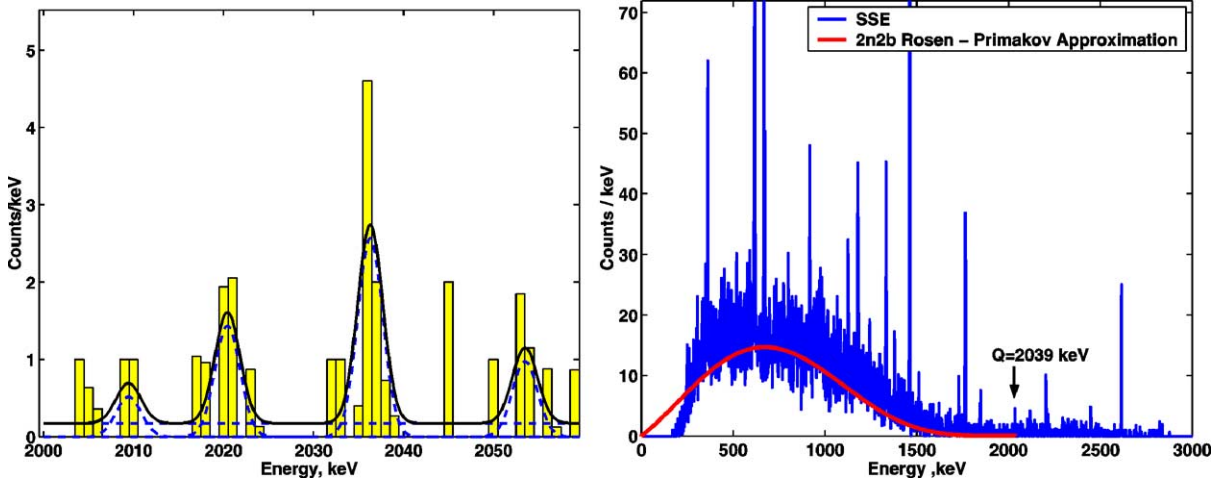
Fig. 9. Left: The pulse shape selected spectrum in the range 2000–2060 keV, taken with detectors 2, 3, 4, 5, in the period 1995–2003 (compare also to Fig. 4 bottom, left). Right: the pulse-shape selected spectrum, selected with the same method as in used in Fig. 8 (top) and in this figure, left part, and for the same measuring period, in the energy range of (100–3000) keV. The solid curve corresponds to the shape of a $2\nu\beta\beta$ spectrum.

by the earlier used PSA methods (for details see [3, 23]). We consider this as an additional proof that we have observed neutrinoless double beta decay. For a detailed discussion see [23].

The energy of the line seen in Figs. 8, 9 is understood to be slightly shifted to lower energy by ballistic effects (see [23]).

The 2039 keV line as a single site events signal cannot be the double escape line of a γ-line whose full energy peak would be expected at 3061 keV where no indication of a line is found in the spectrum measured up to 8 MeV (see [3]). Summarizing, the investigation of $\beta\beta$-like events is proving a line near $Q_{\beta\beta}$ consisting of $0\nu\beta\beta$ events.

11. Half-life of neutrinoless double beta decay of ^{76}Ge

On the basis of the findings presented above we translate the observed number of events into the half-life for neutrinoless double beta decay. In Table 2 we give the half-lives deduced from the full data sets taken in 1995–2003 and in 1990–2003 keV and of some partial data sets, including also the values deduced from the single site spectrum. In the latter case we do conservatively not apply, a calibration factor. Also given are the effective neutrino masses. The result obtained is consistent with the results we reported

in [14,15], and also with the limits given earlier in [5]. Concluding we confirm, with 4.2σ (99.9973% c.l.) probability, our claim from 2001 [14,15] of first evidence for the neutrinoless double beta decay mode.

12. Consequences

Consequence of the above result is, that lepton number is not conserved. Further the neutrino is a Majorana particle see, e.g., [28]. Both of these conclusions are *independent of any* discussion of nuclear matrix elements. The matrix element enters when we derive a *value* for the effective neutrino mass—making the *most natural assumption* that the $0\nu\beta\beta$ decay amplitude is dominated by exchange of a massive Majorana neutrino. The half-life for the neutrinoless decay mode is under this assumption given by [27]

$$\left[T_{1/2}^{0\nu}\left(0_i^+ \to 0_f^+\right)\right]^{-1}$$
$$= C_{mm}\frac{\langle m\rangle^2}{m_e^2} + C_{\eta\eta}\langle\eta\rangle^2 + C_{\lambda\lambda}\langle\lambda\rangle^2$$
$$+ C_{m\eta}\langle\eta\rangle\frac{\langle m\rangle}{m_e} + C_{m\lambda}\langle\lambda\rangle\frac{\langle m_\nu\rangle}{m_e} + C_{\eta\lambda}\langle\eta\rangle\langle\lambda\rangle,$$
$$\langle m\rangle = \left|m_{ee}^{(1)}\right| + e^{i\phi_2}\left|m_{ee}^{(2)}\right| + e^{i\phi_3}\left|m_{ee}^{(3)}\right|,$$

where $m_{ee}^{(i)} \equiv |m_{ee}^{(i)}|\exp(i\phi_i)$ $(i = 1, 2, 3)$ are the contributions to the effective mass $\langle m\rangle$ from in-

Table 2
Half-life for the neutrinoless decay mode and the deduced effective neutrino mass from the HEIDELBERG–MOSCOW experiment (the nuclear matrix element of [27] is used, see text). Shown are in addition to various accumulated total measuring times also the results for four *non-overlapping* data sets: the time periods 11.1995–09.1999 and 09.1999–05.2003 for *all* detectors, and the time period 1995–2003 for two sets of detectors: $1 + 2 + 4$, and $3 + 5$

Significance [kg yr]	Detectors	$T_{1/2}^{0\nu}$ [yr] (3σ range)	$\langle m \rangle$ [eV] (3σ range)	Conf. level (σ)
		Period 1990–2003		
71.7	1, 2, 3, 4, 5	$(0.69–4.18) \times 10^{25}$ 1.19×10^{25} [a]	$(0.24–0.58)$ 0.44 [a]	4.2
		Period 1995–2003		
56.66	1, 2, 3, 4, 5	$(0.67–4.45) \times 10^{25}$ 1.17×10^{25} [a]	$(0.23–0.59)$ 0.45 [a]	4.1
51.39	2, 3, 4, 5	$(0.68–7.3) \times 10^{25}$ 1.25×10^{25} [a]	$(0.18–0.58)$ 0.43 [a]	3.6
42.69	2, 3, 5	$(0.88–4.84) \times 10^{25}$ (2σ range) 1.5×10^{25} [a]	$(0.22–0.51)$ (2σ range) 0.39 [a]	2.9
51.39 (SSE)	2, 3, 4, 5	$(1.04–20.38) \times 10^{25}$ 1.98×10^{25} [a]	$(0.11–0.47)$ 0.34 [a]	3.3
28.21	1, 2, 4	$(0.67–6.56) \times 10^{25}$ (2σ range) 1.22×10^{25} [a]	$(0.19–0.59)$ (2σ range) 0.44 [a]	2.5
28.35	3, 5	$(0.59–4.29) \times 10^{25}$ (2σ range) 1.03×10^{25} [a]	$(0.23–0.63)$ (2σ range) 0.48 [a]	2.6
		Period 1990–2000		
50.57	1, 2, 3, 4, 5	$(0.63–3.48) \times 10^{25}$ 1.24×10^{25} [a]	$(0.08–0.61)$ 0.43 [a]	3.1
		Period 1995–09.1999		
26.59	1, 2, 3, 4, 5	$(0.43–12.28) \times 10^{25}$ 0.84×10^{25} [a]	$(0.14–0.73)$ 0.53 [a]	3.2
		Period 09.1999–05.2003		
30.0	1, 2, 3, 4, 5	$(0.60–8.4) \times 10^{25}$ 1.12×10^{25} [a]	$(0.17–0.63)$ 0.46 [a]	3.5

[a] Denotes best value.

dividual mass eigenstates, with ϕ_i denoting relative Majorana phases connected with CP violation, and $C_{mm}, C_{\eta\eta}, \dots$ denote nuclear matrix elements squared. Ignoring contributions from right-handed weak currents on the right-hand side of the above equation, only the first term remains.

Using the nuclear matrix element from [27], we conclude from the measured half-life given in Table 2

the effective mass $\langle m \rangle$ to be $\langle m \rangle = (0.2–0.6)$ eV (99.73% c.l.). The matrix element given by [27] was the *prediction closest to* the *later* measured $2\nu\beta\beta$ decay half-life of $(1.74^{+0.18}_{-0.16}) \times 10^{21}$ yr [4,9]. It underestimates the 2ν matrix elements by 32% and thus these calculations will also underestimate (to a smaller extent) the matrix element for $0\nu\beta\beta$ decay, and consequently correspondingly overestimate the

(effective) neutrino mass. Allowing conservatively for an uncertainty of the nuclear matrix element of $\pm 50\%$, the range for the effective mass may widen to $\langle m \rangle = (0.1\text{–}0.9)$ eV (99.73% c.l.).

With the value deduced for the effective neutrino mass, the HEIDELBERG–MOSCOW experiment excludes several of the neutrino mass scenarios allowed from present neutrino oscillation experiments (see Fig. 1 in [30])—allowing only for degenerate mass scenarios [42].

Assuming other mechanisms to dominate the $0\nu\beta\beta$ decay amplitude, which have been studied extensively in recent years, the result allows to set stringent limits on parameters of SUSY models, leptoquarks, compositeness, masses of heavy neutrinos, of the right-handed W boson, and possible violation of Lorentz invariance and equivalence principle in the neutrino sector. For a discussion and for references we refer to [1,29].

13. Conclusion and perspectives

Concluding, evidence for a signal at $Q_{\beta\beta}$ on a confidence level of 4.2σ has been observed confirming our earlier claim. On the basis of our pulse shape analysis this can be interpreted as evidence for neutrinoless double beta decay of ^{76}Ge, and thus for *total* lepton number nonconservation, and for a nonvanishing Majorana neutrino mass. Recent information from many *independent* sides seems to condense now to a nonvanishing neutrino mass of the order of the value found by the HEIDELBERG–MOSCOW experiment. This is the case for the results from CMB, LSS, neutrino oscillations, particle theory and cosmology (for a detailed discussion see [3]). To mention a few examples: neutrino oscillations require in the case of degenerate neutrinos common mass eigenvalues of $m > 0.04$ eV. An analysis of CMB, large scale structure and X-ray from clusters of galaxies yields a 'preferred' value for $\sum m_\nu$ of 0.6 eV [31]. WMAP yields $\sum m_\nu < 1.0$ eV [32], SDSS yields $\sum m_\nu < 1.7$ eV [33]. Theoretical papers require degenerate neutrinos with $m > 0.1$ and 0.2 eV [35,36], and the recent alternative cosmological concordance model requires relic neutrinos with mass of order of eV [37]. The Z-burst scenario for ultra-high energy cosmic rays requires $m_\nu \sim 0.4$ eV [38], and also non-standard model $(g-2)$ has been connected with degenerate neutrino

masses >0.2 eV [39]. It has been discussed that the Majorana nature of the neutrino may tell us that spacetime does realize a construct that is central to construction of supersymmetric theories [40].

Looking into the future, there is some hope from the numbers given in Table 2, that the future tritium experiment KATRIN [41] may see a positive signal, if tritium decay can solve this problem at all (see [34]).

From future double beta projects to improve the present accuracy of the effective neutrino mass one has to require that they should be able to differentiate between a β and a γ signal, or that the tracks of the emitted electrons should be measured. At the same time, as is visible from the present information, the energy resolution should be *at least* in the order of that of Ge semiconductor detectors. If one wants to get *independent additional* insight into the neutrinoless double beta decay process, one would probably wish to see the effect in *another* isotope, which would then simultaneously give additional information also on the nuclear matrix elements. In view of the above remarks, future efforts to obtain *deeper* information on the process of neutrinoless double beta decay, would require *a new experimental approach, different from all, what is at present pursued.*

References

[1] H.V. Klapdor-Kleingrothaus (Ed.), 60 Years of Double Beta Decay—From Nuclear Physics to Beyond the Standard Model, World Scientific, Singapore, 2001.

[2] H.V. Klapdor-Kleingrothaus, Proposal, MPI-1987-V17, September 1987.

[3] H.V. Klapdor-Kleingrothaus, A. Dietz, O. Chkvorets, I.V. Krivosheina, Nucl. Instrum. Methods A 522 (2004) 367.

[4] HEIDELBERG–MOSCOW Collaboration, Phys. Rev. D 55 (1997) 54.

[5] H.V. Klapdor-Kleingrothaus, et al., Eur. Phys. J. A 12 (2001) 147, hep-ph/0103062.

[6] Dissertations:
(a) B. Maier, November 1995, MPI-Heidelberg;
(b) F. Petry, November 1995, MPI-Heidelberg;
(c) J. Hellmig, November 1996, MPI-Heidelberg;
(d) B. Majorovits, December 2000, MPI-Heidelberg;
(e) A. Dietz, June 2003, MPI-Heidelberg;
A. Dietz, Dipl. Thesis, Univ. Heidelberg, 2000 (unpublished);
(f) Ch. Dörr, Univ. Heidelberg, 2002 (unpublished).

[7] G. Douysset, et al., Phys. Rev. Lett. 86 (2001) 4259.

[8] J.G. Hykawy, et al., Phys. Rev. Lett. 67 (1991) 1708;
G. Audi, A.H. Wapstra, Nucl. Phys. A 595 (1995) 409;
R.J. Ellis, et al., Nucl. Phys. A 435 (1985) 34.

[9] Ch. Dörr, H.V. Klapdor-Kleingrothaus, Nucl. Instrum. Methods A 513 (2003) 596.

[10] R.B. Firestone, V.S. Shirley (Eds.), Table of Isotopes, eighth ed., Wiley, New York, 1998;
National Nuclear Data Center, Brookhaven National Laboratory, Evaluated Nuclear Structure Data File (ENSDF) http://www.nndc.bnl.gov/nndc/ensdf/.

[11] H.V. Klapdor-Kleingrothaus, O. Chkvorets, I.V. Krivosheina, C. Tomei, Nucl. Instrum. Methods A 511 (2003) 335.

[12] J. Hellmig, H.V. Klapdor-Kleingrothaus, Nucl. Instrum. Methods A 455 (2000) 638;
J. Hellmig, F. Petry, H.V. Klapdor-Kleingrothaus, Patent DE19721323A;
B. Majorovits, H.V. Klapdor-Kleingrothaus, Eur. Phys. J. A 6 (1999) 463.

[13] A.M. Bakalyarov, et al. (Moscow group of HEIDELBERG–MOSCOW experiment), hep-ex/0309016.

[14] H.V. Klapdor-Kleingrothaus, et al., Mod. Phys. Lett. A 16 (2001) 2409.

[15] H.V. Klapdor-Kleingrothaus, A. Dietz, I.V. Krivosheina, Found. Phys. 31 (2002) 1181, and Corrigenda, 2003;
H.V. Klapdor-Kleingrothaus, A. Dietz, I.V. Krivosheina, Part. Nucl. 110 (2002) 57.

[16] H.V. Klapdor-Kleingrothaus, A. Dietz, I.V. Krivosheina, Ch. Dörr, C. Tomei, Nucl. Instrum. Methods A 510 (2003) 281;
H.V. Klapdor-Kleingrothaus, A. Dietz, I.V. Krivosheina, Ch. Dörr, C. Tomei, Phys. Lett. B 578 (2004) 54.

[17] M.D. Hannam, W.J. Thompson, Nucl. Instrum. Methods A 431 (1999) 239.

[18] Yu. Zdesenko, et al., Phys. Lett. B 546 (2002) 206.

[19] Ch.L. Lawson, R.J. Hanson, Solving Least Square Problems, in: Classics in Applied Mathematics, SIAM, Philadelphia, PA, 1995;
D.W. Marquardt, J. Soc. Industr. Appl. Math. 11 (1963) 431;
Ph.R. Bevington, D.K. Robinson, in: Data Reduction and Error Analysis for the Physical Sciences, second ed., McGraw–Hill, New York, 1992, p. 328;

J.C. Lagarias, J.A. Reeds, M.N. Wright, P.E. Wright, SIAM J. Opt. 9 (1) (1998) 112;
T.H. Martin, B.M. Mohammad, IEEE Trans. Neural Networks 5 (1996) 959.

[20] V.B. Zlokazov, preprint JINR-P10-86-502, September 1986 and JINR-P10-88-94, March 1988, JINR, Dubna, Russia.

[21] www.mathworks.com.

[22] http://root.cern.ch/root/html/.

[23] H.V. Klapdor-Kleingrothaus, et al., in preparation.

[24] D.E. Groom, et al., Particle Data Group, Eur. Phys. J. C 15 (2000) 1;
G.J. Feldman, R.D. Cousins, Phys. Rev. D 57 (1998) 3873.

[25] D. Caldwell, J. Phys. G 17 (1991) S137.

[26] A.A. Vasenko, et al., Mod. Phys. Lett. A 5 (1990) 1299;
I. Kirpichnikov, Preprint ITEP (1991).

[27] A. Staudt, K. Muto, H.V. Klapdor-Kleingrothaus, Europhys. Lett. 13 (1990) 31;
K. Muto, E. Bender, H.V. Klapdor, Z. Phys. A 334 (1989) 177.

[28] J. Schechter, J.W.F. Valle, Phys. Rev. D 25 (1982) 2951.

[29] H.V. Klapdor-Kleingrothaus, U. Sarkar, hep-ph/0302237.

[30] H.V. Klapdor-Kleingrothaus, U. Sarkar, Mod. Phys. Lett. A 18 (2003) 2243;
H.V. Klapdor-Kleingrothaus, U. Sarkar, Mod. Phys. Lett. A 16 (2001) 2469;
H.V. Klapdor-Kleingrothaus, H. Päs, A.Yu. Smirnov, Phys. Rev. D 63 (2001) 073005.

[31] S.W. Allen, R.W. Schmidt, S.L. Bridle, astro-ph/0306386.

[32] S. Hannestad, CAP 0305 (2003) 920030, 004, astro-ph/0303076;
Also see, in: H.V. Klapdor-Kleingrothaus (Ed.), Proc. of BEYOND03, Ringberg Castle, Germany, 9–14 June 2003, Springer, Heidelberg, 2003.

[33] M. Tegmark, et al., astro-ph/0310723.

[34] M. Kirchbach, C. Compean, L. Noriega, hep-ph/0310297;
M. Kirchbach, in: H.V. Klapdor-Kleingrothaus (Ed.), Proc. of BEYOND03, 4th Int. Conf. on Particle Physics Beyond the Standard Model, Ringberg Castle, Germany, 9–14 June 2003, Springer, 2004.

[35] K.S. Babu, E. Ma, J.W.F. Valle, Phys. Lett. B 552 (2003) 207, hep-ph/0206292;
E. Ma, hep-ph/0307016; in: H.V. Klapdor-Kleingrothaus (Ed.), Proc. of BEYOND03, 4th Int. Conf. on Particle Physics Beyond the Standard Model, Ringberg Castle, Germany, 9–14 June 2003, Springer, 2004.

[36] R.N. Mohapatra, M.K. Parida, G. Rajasekaran, hep-ph/0301234.

[37] A. Blanchard, M. Douspis, M. Rowan-Robinson, S. Sarkar, astro-ph/0304237.

[38] D. Fargion, et al., in: H.V. Klapdor-Kleingrothaus (Ed.), Proc. of DARK2000, Heidelberg, Germany, July 10–15, 2000, Springer, Berlin, 2001, pp. 455–468;
D. Fargion, et al., in: H.V. Klapdor-Kleingrothaus (Ed.), Proc. of BEYOND02, Oulu, Finland, June 2002, IOP, Bristol, 2003;
D. Fargion, et al., in: BEYOND03, Ringberg Castle, Germany, 9–14 June 2003, Springer, Heidelberg, 2003;
Z. Fodor, S.D. Katz, A. Ringwald, Phys. Rev. Lett. 88 (2002) 171101;

Z. Fodor, et al., JHEP 0206 (2002) 046, hep-ph/0203198;
Z. Fodor, et al., in: H.V. Klapdor-Kleingrothaus (Ed.), Proc. of Beyond the Desert 02, BEYOND'02, Oulu, Finland, 2–7 June 2002, IOP, Bristol, 2003, hep-ph/0210123.

[39] E. Ma, M. Raidal, Phys. Rev. Lett. 87 (2001) 011802, hep-ph/0102255;
E. Ma, M. Raidal, Phys. Rev. Lett. 87 (2001) 159901, Erratum.

[40] D.V. Ahluwalia, in: H.V. Klapdor-Kleingrothaus (Ed.), Proc. of BEYOND'02, Oulu, Finland, 2–7 June, 2002, IOP, Bristol, 2003, pp. 143–160;
D.V. Ahluwalia, M. Kirchbach, Phys. Lett. B 529 (2002) 124.

[41] http://www-ik.fzk.de/%7ekatrin/atw/talks.html;
J. Bonn, et al., Nucl. Phys. B (Proc. Suppl.) 110 (2002) 395.

[42] H.V. Klapdor-Kleingrothaus, in: H.V. Klapdor-Kleingrothaus (Ed.), Proc. BEYOND03, Springer, Heidelberg, 2004.